A tomographic UV-sheet scanning technique for producing 3D fluorescence images of x-ray beams in a radio-fluorogenic gel

Yao, Tiantian; Gasparini, Alessia; de Haas, Thijs; Luthjens, Lee; Denkova, Antonia; Warman, John

DOI
10.1088/2057-1976/aa684b

Publication date
2017

Document Version
Final published version

Published in
Biomedical Physics & Engineering Express

NOTE • OPEN ACCESS

A tomographic UV-sheet scanning technique for producing 3D fluorescence images of x-ray beams in a radio-fluorogenic gel

To cite this article: Tiantian Yao *et al* 2017 *Biomed. Phys. Eng. Express* **3** 027004

Biomedical Physics & Engineering Express

NOTE

A tomographic UV-sheet scanning technique for producing 3D fluorescence images of x-ray beams in a radio-fluorogenic gel

Tiantian Yao, Alessia Gasparini, Matthijs P De Haas, Leonard H Luthjens, Antonia G Denkova and John M Warman

Delft University of Technology, Faculty of Applied Sciences, Department of Radiation Science and Technology, Section Radiation and Isotopes for Health, Mekelweg 15, 2629 JB DELFT, The Netherlands

E-mail: J.M.Warman@TUDelft.nl

Keywords: 3D dosimetry, polymer gel dosimetry, radiofluorogenic gels, fluorescence tomography, 3D imaging

Supplementary material for this article is available online

OPEN ACCESS

RECEIVED
1 February 2017

REVISED
1 March 2017

ACCEPTED FOR PUBLICATION
22 March 2017

PUBLISHED
11 April 2017

Abstract

In this work a 40 mm cube of an optically clear, radio-fluorogenic gel composed of partially-polymerized tertiary-butyl acrylate and maleimido-pyrene (~0.01%) is irradiated with orthogonally-crossed, 10 mm square and round, 200 kVp x-ray beams. A thin sheet of UV light is produced between two parallel plates with 2 mm slits illuminated by collimated, linear-array, LED sources. The gel is transported 1 mm at a time through the UV sheet and the fluorescence from the emissive, polymeric radiolytic product formed in the x-ray tracks is recorded, as both JPEG and raw-DNG files, using a CCD camera placed orthogonal to the plane of the excitation light. The resulting stack of 40 tomographic slices are imported into freely-available software to produce 3D animated images of the radiation-induced fluorescence.

1. Introduction

A method capable of monitoring the energy deposited by ionizing-radiation in three-dimensions with (sub) millimeter spatial resolution is a longstanding wish of clinical radiation physicists for quality assurance (QA) auditing of the increasingly complex computer-designed protocols used for patient treatment (Ibbott and Thwaites 2015, Kron *et al* 2016). A variety of methods aimed at fulfilling this wish have been proposed and have been reviewed by Baldock *et al* (2010), Jordan (2010), Vandecasteele and De Deene (2013), and more recently by Schreiner (2015), Oldham (2015) and Beaulieu and Beddar (2016). Despite the tremendous research effort illustrated in these reviews and the large volume of publications of research presented at the international DosGel/3DDose conferences held since 1999, general acceptance in the clinic has been disappointing.

We present here recent results of a method not previously reviewed that is capable of providing fluorescent 3D images of complex radiation fields with submillimetre spatial resolution (Warman *et al* 2011, 2013). The method is based on radio-fluorogenic (RFG) co-polymerization by which a *fixed* fluorescent image of a complex radiation field is produced within an otherwise clear and tissue-equivalent gel. In this report we demonstrate how the three-dimensional fluorescent image created in such a gel by orthogonally-crossed round and square x-ray beams can be reconstructed using a tomographic fluorescence scanning technique. The simplicity of the two-component gel formulation and the data acquisition equipment could possibly reduce some of the barriers to clinical acceptance. The results reported are taken from chapter 7 of the PhD thesis of Yao (2017).

2. Materials and methods

The RFG gel used was composed of 15% pre-polymerized tertiary-butyl acrylate (TBA) containing approximately 0.01% of the fluorogenic compound maleimido-pyrene (MPy). For details of the molecular structures, reaction mechanism and gel preparation see Warman *et al* (2011) and Yao (2017 chapter 5). In the work reported here, approximately 70 ml of an RFG gel was prepared in a 40 × 40 mm^2 square cell as shown in figure 1. The gel has a density of 0.91 $kg\,l^{-1}$ and is composed only of the light elements H, O, C and

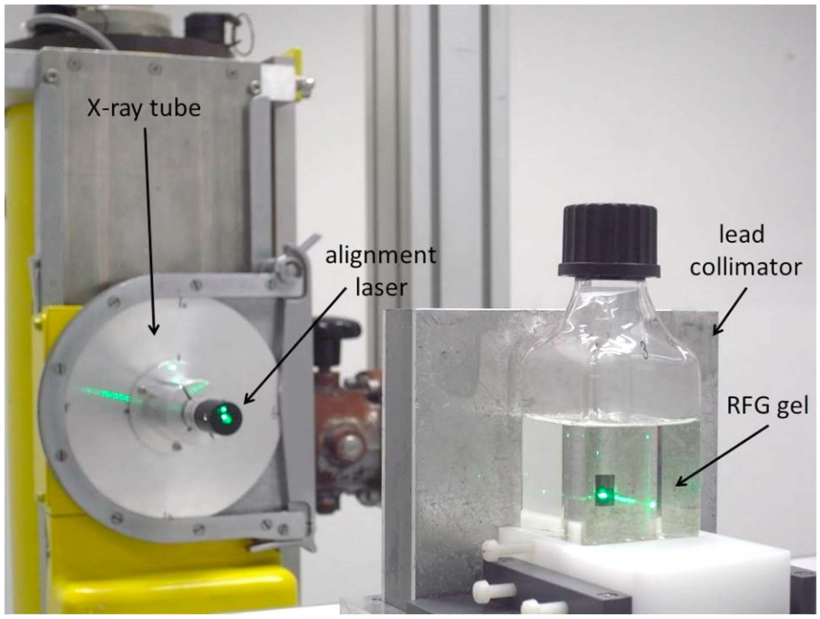

Figure 1. The x-ray apparatus with a 10 mm square lead collimator in front of a 40 mm i.d. square cell containing the RFG gel on an optical rail with a laser beam for alignment.

N with a molecular structure similar to that of PMMA, which is frequently used as a 'solid water' substitute. The basic TBA gel is optically clear with a transmittance of greater than 95% down to the acrylate absorption edge at 315 nm even after 15% polymer conversion (Yao *et al* 2014, Yao 2017 figure 2.8). There is no evidence for a decrease in the transmittance due to light scattering resulting from turbidity on irradiation as often occurs in aqueous polymer gels.

The gel was irradiated with 200 kVp x-rays from a Philips MCN 321 x-ray tube. The x-ray beam was collimated by either a 10 mm square or round aperture in a 21 mm thick lead plate on an optical bench and aligned using an alignment laser (Laserglow Technologies,'Galileo PRO') as shown in figure 1. In this paper the gel was irradiated first with a square beam and subsequently with a round beam with the cell turned through 90°. In both cases the cell was irradiated at an SSD of 50 cm for 20 min with an incident dose rate of 0.94 Gy min^{-1} determined with Gafchromic MD-V3 radiochromic film attached to the cell. The MD-V3 film was calibrated for 200 kVp x-rays using an ionization chamber that is annually checked at the Netherlands Metrology Institute (Yao *et al* 2016, Yao 2017 chapter 6).

Fundamental studies of the physico–chemical changes in an RFG solution or gel have been carried out using 10 or 20 mm square cells irradiated in cobalt-60 cavity sources (Yao 2017 chapters 2, 3, 4 and 5). In these GC200 and GC220 sources the dose rates were uniform within 2% over the whole cell volume (Smith and Lee 1996).

Measurement of the fluorescence of the irradiated gel was made using the 'sheet-scanning' equipment shown schematically in figure 2. The ultraviolet light sources (from 4PICO.NL) consisted of 16 cm long, linear arrays of 22 light emitting diodes with a rectangular Fresnel lens for beam collimation and a 1 mm thick UG1 filter ('Woods glass' from Schott) to attenuate any visible wavelength components of the LED emission with $\lambda_{max} = 381 \pm 5$ nm. The UV excitation light was restricted to a vertical sheet between two 3 mm thick Al plates by 2 mm slits for beam transmission. A cell containing a micromolar solution of the fluorescence standard diphenylanthracene in cyclohexane is routinely used as an actinometer to check the intensity and uniformity of the UV illumination along the *y*-axis (Yao 2017 p 58; Warman *et al* 2011). The optical density of the RFG gel at the excitation wavelength was 0.30 ((MPy) = 0.30 mM, $\varepsilon_{381} = 250\,l\,mol^{-1}\,cm^{-1}$). This results in a 6% dip in the intensity at the center of the cell on the *x*-axis (Yao 2017 p 60).

The cell containing the irradiated gel was placed on a translation stage that allowed it to be transported past the slits and through the illuminating sheet of UV light. Images of the fluorescence were taken using a CCD camera (Ricoh GX200) as a function of the slit position with respect to the front face of the gel, '*z*' in figure 2. For the results presented here translation of the cell was carried out manually, in 1 mm steps, using a micrometer drive. The resulting 40 JPEG and raw DNG images (tomographic slices) were imported into ImageJ for data processing. The DNG pixel levels have been shown to be linearly dependent on photon exposure over the ranges studied (Yao 2017 figure 3.10). The pixel spatial resolution changes linearly from 54 to 65 pixels mm^{-1} with increasing *z* (Yao 2017 p 153 and figure 7.13)

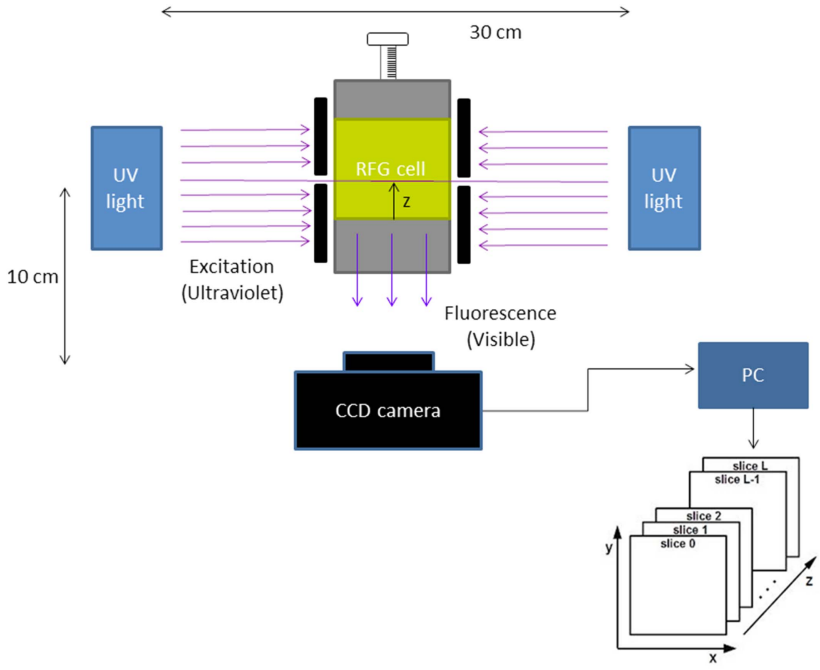

Figure 2. A schematic of the sheet-scanning apparatus used for making stacks of tomographic fluorescent slices. An animated version of the figure is available in the supplemental information.

In ImageJ the files were split into their separate red, green and blue pixel channels using the 'Image/Color/Split Channels' function. Since the fluorescence of the gel lies mainly in the blue ($\lambda_{max} \sim 400$ nm), the blue component was used for image visualization (JPEG) and quantification (DNG). Bright and dark outliers were removed using the function 'Process/Noise/Remove Outliers'. The images were then stacked in the z direction using the 'Image/Stacks/Images to Stack' function, and the stack was saved. The 'depth-cue parameters' (spatial dimensions) width, height and voxel depth required to produce the perspective of the 3D projections were set under 'Image/Properties'. The pixel levels between slices were taken to be the average value of the two adjacent slices. 3D volume or ortho-slice (cross-section) views could be reconstructed from a given stack using the '3D Viewer' plug-in (https://imagej.nih.gov/ij/plugins/3d-viewer/) under 'Plugins/3D/3D Viewer'. The volume rendering in ImageJ using the procedure outlined above displays only the surface of the fluorescent volume; intensity variations within the volume cannot be seen.

To produce 3D volume renderings that do display the internal intensity variations we imported the stacked JPEG images saved in ImageJ into the image-processing platform BioImageXD (Kankaanpää *et al* 2012) (http://bioimagexd.net/). This volume rendering uses pixel transparency to create semi-translucent structures in which a parameter α represents the opacity of the pixels (Rueden and Eliceiri 2007). The pixel transparency reveals the structures beneath the outer surface of the volume.

3. Results and discussion

In figure 3 (upper) the gel transport trajectories are illustrated (top view) for scans along the z-axis of the round (scan 1) and the square (scan 2) beams achieved by simply turning the cell through 90°. Samples of individual x–y plane fluorescent slices obtained at selected values of the translation distance z are shown in the lower part of the figure. Time-lapse movies derived from all 40 slices are included in the supplementary information is available online at stacks.iop.org/BPEX/3/027004/mmedia. In the scans one can clearly see the difference between the suddenness of a square beam crossing a round beam and the gradualness of a round beam crossing a square beam. The actual geometry of the energy deposition at the junction of the beams is quite complex even for this relatively simple case.

The 3D renderings of the fluorescence shown in figure 4 were derived using only the slices from scan 1. On the left of the figure is the *envelope* image obtained using ImageJ and on the right the *translucent* image obtained using BioImageXD. Both images can be manually rotated or allowed to freely rotate to produce a movie version as shown in the supplementary information. For providing these animated, visual representations the JPEG files we used. For quantitative, linear-intensity data analysis the much larger raw DNG files are used together with $x/y/z$ slices through the 3D structures.

The spatial resolution of the images shown in figure 4 is difficult to define since in the x–y plane of the tomographic slices the limit to the resolution is

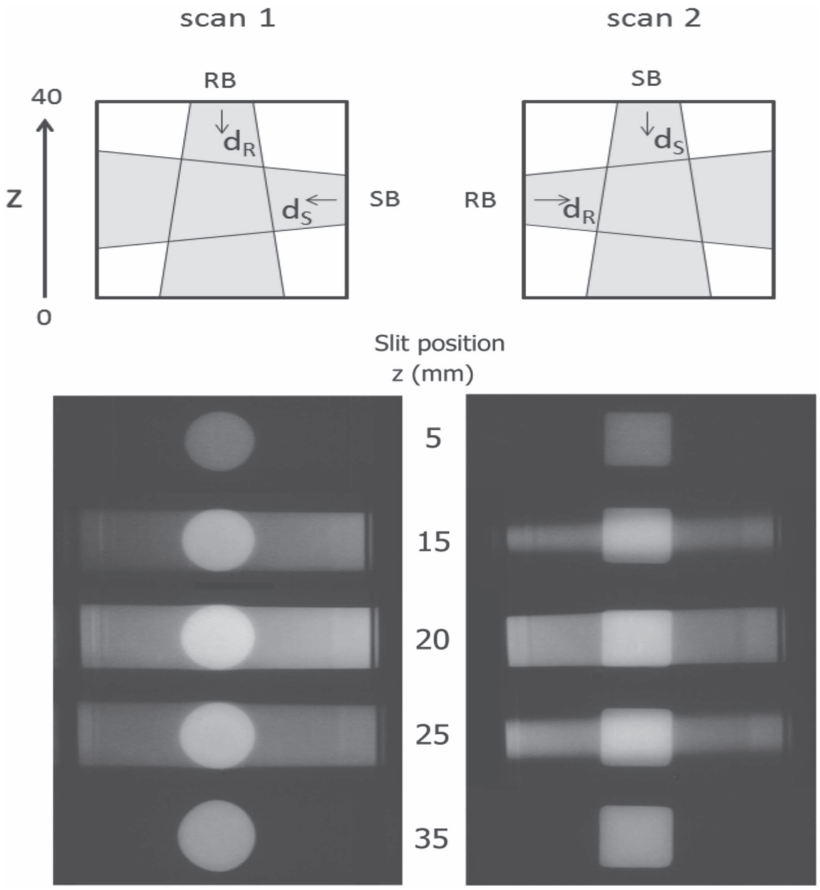

Figure 3. Upper: schematic drawings (top view, x–z plane at $y = 20$ mm) of the geometries of the x-ray beams corresponding to the conditions of scans 1 and 2 with d_R and d_S the penetration depths of the round and square beams respectively. The beam divergences with depth have been exaggerated in the diagram. Lower: blue pixel level images of the fluorescence from x–y plane slices of the irradiated RFG gel taken at the specific z values shown for scan 1 (left) and scan 2 (right). All 40 slices can be viewed in a time-lapse or fly-through animation of the scanning process in the supplementary information.

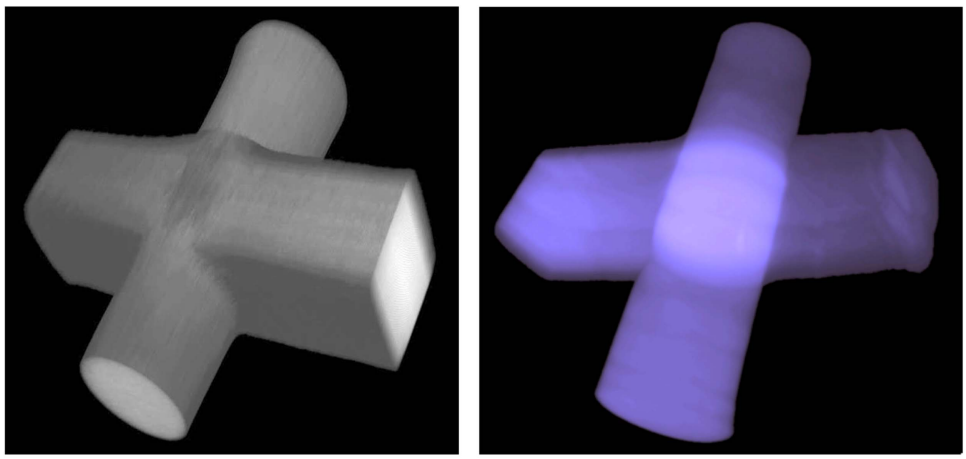

Figure 4. Left: A three-dimensional *envelope* reconstruction of the crossed x-ray beams using '3D Viewer' in ImageJ from the stack of 40 slices taken as illustrated in scan 1 shown in figure 3, i.e. along the axis of the round beam. Right: a three-dimensional *translucent* reconstruction of the crossed x-ray beams using 'BioImageXD' with the same stack of slices. Movies of both reconstructions can be found in the supplementary information.

determined by the effective inter-pixel distance of approximately 0.02 mm while in the z-direction the resolution will be determined by the 2 mm slit width and the 1 mm translation steps. From transverse scans of an image of the square beam in the x–y plane at $z = 20$ mm, the 20%–80% rise and fall distance ('penumbra') has been measured to be 0.67 and 0.94 mm at depths of 5 and 35 mm in the gel (Yao,

p152). These values lie between those of 0.43 and 0.96 mm determined for the incident and exit beam penumbra using radio-chromic film attached to the front and back of the cell (Yao 2017 p 146). For penumbra measurements profile scans were made using the DNG images for which the pixel level is linearly dependent on the fluorescence intensity (Yao 2017 figure 3.10). For purposes of visualization and animation, as in figure 4, the much smaller JPEG files were used.

4. Conclusion

We show that it is possible to produce animated 3D images of the fluorescence induced in a RFG gel on irradiation with a complex radiation field. The method uses a simple, inexpensive UV-sheet scanning technique to produce tomographic slices of the gel fluorescence. The stack of slices is then imported into the freely-available software platforms ImageJ or BioImageXD to produce 3D envelope or translucent animated images. Immediate post-irradiation data collection and analysis is possible. In the present work scanning was carried out manually. A prototype of a fully-automated apparatus with direct read-out is being tested.

While the raw DNG pixel levels provide a linear representation of the actual fluorescence intensity of a given slice, corrections are necessary to produce an image that is proportional to the concentration of the emissive radiolytic product. This should take into account the (in the present case 6%) dip in the UV intensity along the *x*-axis due to absorption of the UV excitation light (Yao 2017 p 60); the slight non-uniformity in the UV intensity along the *y*-axis (Yao 2017 p 58); and the change in the spatial pixel resolution with position along the *z*-axis (Yao 2017 p 153). We are in the process of making these corrections using MatLab to modify individual slices prior to assembly.

To be applicable as a 3D dosimeter the relationship between the concentration of the emissive product formed and the (calorimetric) energy deposited must be determined. This requires an understanding of the radiation chemical foundation of the product formation, which is a *sine qua non* for all chemically-based dosimeters (Chorzempa 1970). To this end we have carried out an extensive study of the parameters influencing the co-polymerization of MPy in a TBA matrix and have derived a reaction mechanism that explains these observations (Yao 2017 p 72). This can be used to determine algorithms relating the product yield to the parameters accumulated dose, dose rate and concentration of the fluorogenic compound (Yao 2017 chapters 3 and 5). In future work we will apply these algorithms to the data in order to obtain images that are proportional to the local dose and/or dose rate in an RFG gel medium. The present measurements are clearly just the first step in the production of a 3D dosimeter based on radiation-induced fluorescence in a RFG gel.

References

Baldock C, De Deene Y, Doran S, Ibbott G, Jirasek A, Lepage M, McAuley K B, Oldham M and Schreiner L J 2010 Polymer gel dosimetry *Phys. Med. Biol.* **55** R1–63

Beaulieu L and Beddar S 2016 Review of plastic and liquid scintillation dosimetry for photon, electron, and proton therapy *Phys. Med. Biol.* **61** R305–43

Chorzempa M A 1970 Ionizing radiation and its chemical effects: a historical study of chemical dosimetry (1902–1962) *PhD Thesis* University of Oregon (http://ir.library.oregonstate.edu/xmlui/bitstream/handle/1957/45710/ChorzempaSisterM1971.pdf;sequence=3)

Ibbott G S and Thwaites D I 2015 Audits for advanced treatment dosimetry *J. Phys.: Conf. Ser.* **573** 012002

Jordan K 2010 Review of recent advances in radiochromic materials for 3D dosimetry *J. Phys.: Conf. Ser.* **250** 012043

Kankaanpää P, Paavolainen L, Tiitta S, Karjalainen M, Päivärinne J, Nieminen J, Marjomäki V, Heino J and White D J 2012 BioImageXD: an open, general-purpose and high-throughput image-processing platform *Nat. Methods* **9** 683–9

Kron T, Lehmann J and Greer P 2016 Dosimetry of ionising radiation in modern radiation oncology *Phys. Med. Biol.* **61** R167–205

Oldham M 2015 Radiochromic 3D detectors *J. Phys.: Conf. Ser.* **573** 012006

Rueden C T and Eliceiri K W 2007 Visualization approaches for multidimensional biological image data *Biotechniques* **43** 33–6

Schreiner L J 2015 True 3D chemical dosimetry (gels, plastics): development and clinical role *J. Phys.: Conf. Ser.* **573** 012003

Smith B P and Lee P E 1996 A description of ^{60}Co gamma irradiation facilities in the radiation biology and health physics branch *report nr AECL-11567* Atomic Energy of Canada Limited, Chalk River, Ontario, Canada

Vandecasteele J and De Deene Y 2013 Evaluation of radiochromic gel dosimetry and polymer gel dosimetry in a clinical dose verification *Phys. Med. Biol.* **58** 6241–52

Warman J M, de Haas M P, Luthjens L H, Denkova A G, Kavatsyuk O, van Gothem M-J, Kiewiet H H and Brandenburg S 2013 Fixed fluorescent images of an 80 MeV proton pencil beam *Rad. Phys. Chem.* **85** 179–83

Warman J M, Luthjens L H and de Haas M P 2011 High-energy radiation monitoring based on radio-fluorogenic co-polymerization: II. Fixed fluorescent images of collimated x-ray beams using an RFCP gel *Phys. Med. Biol.* **56** 1487–508

Yao T 2017 3D radiation dosimetry using a radio-fluorogenic gel *PhD Thesis* Technische Universiteit Delft (https://doi.org/10.4233/uuid:e8590e7e-944c-4b4c-bc2b-3843400a9f85)

Yao T, Denkova A G and Warman J M 2014 Polymer-gel formation and reformation on irradiation of tertiary-butyl acrylate *Rad. Phys. Chem.* **97** 147–52

Yao T, Luthjens L H, Gasparini A and Warman J M 2016 A study of four radiochromic films currently used for (2D) radiation dosimetry *Rad. Phys. Chem.* **133** 37–44